

# Phase Transitions, Curve Evolution, and the Control of Semiconductor Manufacturing Processes

Jordan Berg  
Institute of Mathematics and Its Applications  
University of Minnesota  
Minneapolis, MN 55455  
jberg@ima.umn.edu

Anthony Yezzi and Allen Tannenbaum  
Department of Electrical Engineering  
University of Minnesota  
Minneapolis, MN 55455  
tannenba@ee.umn.edu

## Abstract

This paper presents a strategy for the estimation and control of certain semiconductor manufacturing processes, employing models developed to describe the dynamics of material interfaces in phase transition problems. Previous work has successfully applied similar models to predict surface evolution in etching and deposition. Here, we propose to adapt these techniques to real-time process monitoring and control. The testbed for algorithm development is a highly simplified model of a plasma etch. Key elements of the scheme are investigated, and found to be feasible.

## 1 Introduction

Given a material that may exist in either of two phases, how will the boundaries between the phases evolve? This is a fundamental question of phase transition physics. One way of mathematically representing phase transition, and investigating these issues, is through an *order parameter*,  $\Phi$ . The value of  $\Phi$  at any point indicates the state of the material, with (for example) zero corresponding to one of the phases, unity to the other. Analysis of the transition dynamics proceeds by allowing  $\Phi$  to vary continuously, without concern for the physical meaning of intermediate values. Then the following parabolic *phase field* equation is an expression of energy minimization for many important physical processes:

$$\Phi_t = \epsilon \Delta \Phi + (1/\epsilon)W'(\Phi) \quad (1)$$

where  $W$  is a double-well potential (in some cases,  $W$  may depend on  $\epsilon$ ), with a local minimum at one and another at zero—that is, the local minima correspond to the two phases. As  $\epsilon$  goes to zero, the domain will typically split into distinct subdomains, with  $\Phi$  tending to values of zero or one in each—except in boundary regions, where one phase smoothly transitions to the

other. The width of these boundary regions goes to zero with  $\epsilon$ . Thus a sharp interface is obtained, in the limit. The motion of the sharp interface may be studied through the limiting behavior of Eq. (1). Its normal velocity, that is, its velocity projected along the normal to the interface, turns out to be given by the sum of two terms. One term, expressing surface energy effects, is related to the *curvature* of the interface. The other, driving the system from a high energy phase to a low energy phase, is a constant *inflationary* term, which vanishes if the values of  $W$  at the local minima are equal. In most physical situations, the curvature term tends to reduce the interface area, while the inflationary contribution may take either sign. Limiting models of this type include the Allen-Cahn antiphase boundary model, the Stefan problem, the Hele-Shaw model, dendritic solidification, and thermal grooving. Kichenassamy, *et al.*, present a detailed discussion of phase field equations, together with a large set of references to which we refer the interested reader [7].

Although Eq. (1) gives insight into the behavior of the phase transition problem, it is not necessary to work with it directly. Rather, one can write down the equations of motion of the evolving interface. In two dimensions, these are the equations of *curve evolution*. Here, a sharp interface is described by a family of parameterized curves,  $C : [0, 1] \times [0, t_f] \rightarrow R^2$ . The curve describing the interface evolves according to,

$$\frac{\partial C}{\partial t} = \alpha(p, t)\mathcal{T} + \hat{\beta}(p, t)\mathcal{N} \quad (2)$$

where  $p$  parametrizes the curve,  $\mathcal{N}$  is the normal,  $\mathcal{T}$  is the tangent, and  $\alpha$ ,  $\beta$  are velocity functions. Changing  $\alpha$  changes only the curve's parametrization, and not its shape. Since we are interested in shape only we may take  $\alpha = 0$ . Much of the mathematical literature considers the special case where the motion is determined solely by the local geometry of the curve. This leads to the following equation:

$$\frac{\partial C}{\partial t} = [\beta_0 + \beta(\kappa)]\mathcal{N}. \quad (3)$$

where  $\kappa(p, t)$  is the curvature, and  $\beta_0$  denotes the constant “inflationary” contribution. For a rigorous formal

<sup>1</sup>This work was supported in part by grants from the National Science Foundation ECS-9122106, by the Air Force Office of Scientific Research AF/F49620-94-1-0058DEF, and by the Army Research Office DAAH04-94-G-0054, DAAH04-93-G-0332.

treatment, as well as a look at some velocity functions of special interest, see [3, 4, 5, 8, 15, 16, 17].

Numerical solution of curve evolution problems can be difficult, for several reasons. One is that, if curvature terms are absent or small, the solution will typically develop corners, or “shocks,” even if the initial data is smooth. Solving for the curve motion after a shock develops—in fact, just giving meaning to such a notion—requires that some form of weak solution be defined, along with associated entropy conditions or viscosity solutions to ensure uniqueness. Another difficulty arises in treating topological transitions of the evolving curve, such as arise when curves merge or split. A series of algorithms that successfully address both these problems have been developed by Osher and Sethian, and their coworkers, based on techniques for *hyperbolic conservation laws* [12, 13, 16]. These algorithms, based on a *level set* representation of the interface, form the basis for our approach.

A number of studies have shown that incorporating feedback control into the the plasma etching process can improve the result [2, 11, 14]. Here we are interested in using *in situ* measurements for real-time control of process parameters. The central problem we address is estimating the evolving shape of the surface features from available measurements. This is a challenging task, but the potential benefits are large. Ultimately, the performance of the finished device will be heavily determined by the surface morphology. This goal is completely complementary to other process control tasks, such as the control of plasma variables.

The idea of applying the theory of curve evolution for modeling etching interfaces in reactive-etching processes has been considered by a number of authors, in particular Shaqfeh and Jurgensen [18], and Singh, *et al.* [19]. Adalsteinsson and Sethian build on this methodology, and apply level set evolution methods to etching, deposition, and lithography [1]. (See also Katardjiev *et al.* for a discussion of curvature dependent flows and level sets in plasma etching [6].) The present work, which emphasizes the use of such models as the basis for real-time estimation, owes a great deal to the efforts of these researchers. Finally, work that attacks a similar real-time interface estimation and control problem (for crystal growth) through an entirely different method has been presented by Srinivasan, *et al.* [22].

The authors would like to thank Pramod Khargonekar for his very helpful information on the control literature in the area of semiconductor manufacturing. Also we would like to thank Jack and Ted Higman for very enlightening conversations on thin-film processing.

## 2 Curvature Flows and Interface Evolution

Let us discuss some properties of Eq. (3), in particular those that give rise to difficulties in analyzing the motion. In what follows, for the curve  $C(t) := (x(p, t), y(p, t))$ ,  $\rho(p, t)$  will denote the metric,  $[x_p^2 + y_p^2]^{1/2}$ , and  $s(p, t)$  the Euclidean arc-length parameter,  $\int_0^p \rho(\zeta, t) d\zeta$ . Note that the total length of the curve is just  $L(t) = s(1, t)$ . The tangent, curvature, and normal, are defined in the standard way [9]. Finally, we let

$$K(t) := \int_0^1 \kappa(p, t) \rho(p, t) dp \quad (4)$$

denote the *total curvature*, and

$$\bar{\kappa}(t) := \int_0^1 |\kappa(p, t)| \rho(p, t) dp \quad (5)$$

denote the *total absolute curvature*.

### 2.1 Hyperbolic Conservation Laws

In principle, corners can form only when curvature terms are absent. In practice, the curvature can become extremely large, and cause numerical problems, even when these terms are nonzero. However, the causes and handling of shocks is best understood by studying the special case where  $\beta(\kappa) = 0$ . Here in the classical manner we will derive a hyperbolic conservation law [16].

Without loss of generality, let  $\beta_0 = 1$ . Then,

$$x_t = \frac{y_p}{(x_p^2 + y_p^2)^{1/2}}; \quad y_t = -\frac{x_p}{(x_p^2 + y_p^2)^{1/2}}. \quad (6)$$

From Eqns. (6) we can derive a hyperbolic conservation law. As long as  $C$  stays smooth and non-self-intersecting, by virtue of the implicit function theorem, we can express the front in the form  $y = U(t, x)$ . Then  $U$  satisfies the Hamilton-Jacobi equation

$$\frac{\partial U}{\partial t} - (1 + U_x^2)^{1/2} = 0. \quad (7)$$

Set  $u := \partial U / \partial x$ . Differentiating (7) with respect to  $x$ , we see that

$$u_t - \left( (1 + u^2)^{1/2} \right)_x = 0. \quad (8)$$

which has the form of a hyperbolic conservation law. It is of interest to note that the conserved quantity is the slope,  $\partial y / \partial x$ . There is a huge classical and modern literature devoted to equations of this type; see [20] and the references therein.

Geometrically, it is very easy to see how discontinuities develop for the system (6). Indeed, it is easy to compute that the curvature satisfies the evolution equation,  $\kappa_t = -\kappa^2$ , which we explicitly solve, to find that

$$\kappa(p, t) = \frac{\kappa(p, 0)}{1 + t\kappa(p, 0)}. \quad (9)$$

Notice that if the initial curve is anywhere concave, i.e., has curvature negative at any point,  $\kappa$  will blow up in finite time, and the resulting curve will develop a singularity, referred to as a *shock* [15].

Once a shock occurs, one must be careful in defining precisely what one means by a “solution” to (8). The answer will depend on the underlying physics of the problem. In geometric optics, nonconvex wavefronts can be handled by the Huygens principle, which defines the propagating front as the *envelope* of a continuum of circles, centered on the initial front. This construction selects a *unique* solution from the many that satisfy the weak form of the eikonal equation. A similar issue arises in solving the Euler equations of compressible flow. Here the notion of viscosity solution naturally arises. Viscosity solutions may be defined for curvature flows as well, with curvature playing the role of viscosity. For curve evolution with constant  $\beta$ , the viscosity solution coincides with the entropy condition imposed in [16], interpreting the hyperbolic evolution law in the prairie-fire sense that “*once a particle is burnt, it stays burnt.*”

## 2.2 Level Set Representations

We now briefly discuss some of the numerical algorithms developed for curve evolution. This work is based on writing the approximations in *conservation form* and applying the *Godunov method* [10]. For more details, see the fundamental work of Osher and Sethian in [12, 13, 16].

Let  $C(p, t)$  satisfy the following evolution equation:

$$\frac{\partial C}{\partial t} = \beta(\kappa)\mathcal{N}. \quad (10)$$

In numerical implementations, the evolving curve is embedded in a two dimensional surface, and then the equations of motion are solved using a combination of straightforward discretization, and numerical techniques derived from hyperbolic conservation laws and Hamilton-Jacobi theory [16, 21].

The embedding step is done in the following manner: The curve  $C(p, t)$  is represented by the zero level set of a smooth and Lipschitz continuous function  $\Phi : R^2 \times [0, \tau] \rightarrow R$ . Assume that  $\Phi$  is negative in the interior and positive in the exterior of the zero level set. We consider the zero level set, defined by

$$\{X(t) \in R^2 : \Phi(X, t) = 0\}. \quad (11)$$

We have to find an evolution equation of  $\Phi$ , such that the evolving curve  $C(t)$  is given by the evolving zero level  $X(t)$ , i.e.,

$$C(t) \equiv X(t). \quad (12)$$

By differentiating (11) with respect to  $t$  we obtain:

$$\nabla\Phi(X, t) \cdot X_t + \Phi_t(X, t) = 0. \quad (13)$$

Note that for the zero level, the following relation holds:

$$\nabla\Phi / \|\nabla\Phi\| = \mathcal{N} \quad (14)$$

In this equation, the left side uses terms of the surface  $\Phi$ , while the right side is related to the curve  $C$ . The combination of equations (10) to (14) gives

$$\Phi_t + \beta(\kappa) \|\nabla\Phi\| = 0 \quad (15)$$

and the curve  $C$ , evolving according to (10), is obtained by the zero level set of the function  $\Phi$ , which evolves according to (15).

The second step of the algorithm consists of the discretization of the equation (15). If singularities cannot develop during the evolution, as in the geometric heat equation flow, a straightforward discretization can be performed [13]. For the types of velocity functions that arise in etching problems, the implementation of the evolution of  $\Phi$  is based on a *monotone* and *conservative* numerical algorithm [10, 13, 21]. For a large class of functions  $\beta$ , such numerical schemes automatically obey the entropy condition corresponding to the Huygens principle [16, 21].

## 3 Estimation and Control of Etching

Semiconductor manufacturing processes are well-suited for the level set techniques described above. The entropy condition has a clear physical interpretation: *material that is removed is never restored*. Some other features of level sets are the ease with which they can be extended from two space dimensions to three, and the potential for capturing effects like surface diffusion in a curvature term. These issues, and others, are discussed extensively in the work [6, 17, 18, 19].

Equation (15) is a completely general description of curve or surface evolution. The physics of the underlying process is entirely contained in the function  $\beta$ . So far,  $\beta$  has been given as a function of curvature only. A realistic description of manufacturing processes for thin-film devices may require that  $\beta$  have a more complicated functional dependence. One possibility is that it will depend on other quantities intrinsic to the interface, such as the direction of the unit normal, or derivatives of the curvature. These flows can be treated by similar methods. It also may occur that the interface normal velocity is determined in part by inherently non-local effects. Some non-local contributions that play a role in low pressure deposition and etching processes are treated by Adalsteinsson and Sethian [1, 17].

### 3.1 Isotropic Etching of a Long Trench

This section describes a highly simplified model of a plasma etching process. Figure 1 depicts the feature

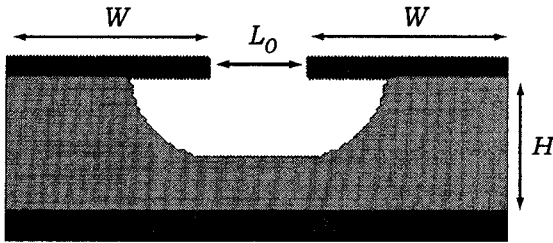


Figure 1: Simplified 2-D Etching Geometry

geometry. A uniform layer of silicon sits on an inert substrate. The silicon is masked with a thin layer of resist, except for a narrow gap. The silicon surface is initially planar, with a uniform height of  $H$ . At  $t = 0$ , a reactive substance, chlorine gas for example, is introduced at the surface. This substance etchs silicon, but not the resist or the substrate. The simplifying assumptions are as follows:

1. The feature to be etched is a trench, very long compared to its width. This allows a 2-D planar approximation.
2. A large number of identical, evenly-spaced, trenches are to be etched. Then only one such may be considered, with periodic boundary conditions.
3. The etch is isotropic. Although isotropic plasma etching is rare, we begin with the isotropic case because an analytical solution is available as a truth model.
4. The etch rate is constant and homogeneous within the material to be etched. For simulation this etch rate is set to one.
5. The mask and substrate are perfectly inert, with an etch rate of zero.

It remains to define an appropriate measurement. Here we consider a measurement of the *total* etch rate, that is, the total quantity of material removed, per unit time. A complete model of the system is then given by Eqns. (11) and (15), and the measurement,

$$y(t) := \int_{X(t)} \chi_e \beta dl \quad (16)$$

The expression (16) is just the normal velocity, integrated over the surface being etched. The characteristic function  $\chi_e$  is needed to distinguish between those parts of the surface that are masked or inert, and those that are actually being etched. Thus, (16) is the amount of material being removed per unit time. It is also the amount of material being released into the surroundings per unit time, and so can be related to the rate

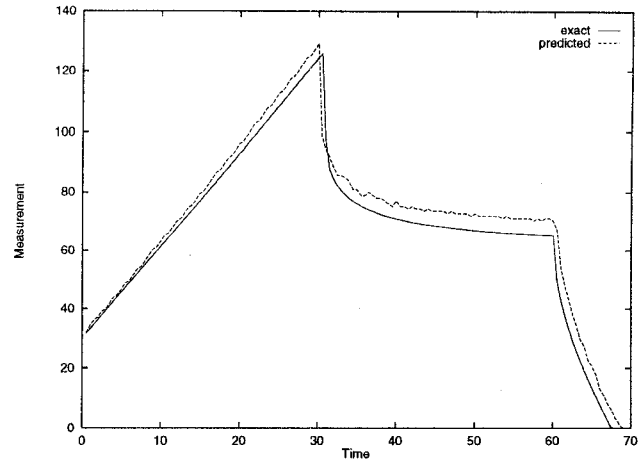


Figure 2: Exact and Predicted Output

of change of concentration. Preliminary experimental work using a chlorine etch of a crystalline silicon wafer suggests that the appropriate concentration can be measured, via optical emission spectroscopy. Note that it is impossible to relate this to the surface velocity without knowledge of the surface shape. Under the above assumptions, the predicted measurement is  $\beta L(t; \beta)$  where  $L(t; \beta)$  is the length of the etching portion of the estimated surface, and the dependence of the time history of  $L$  on  $\beta$  is explicitly indicated. An exact solution is available, using the Huygens principle. The corresponding measurement is,

$$y(t) = \begin{cases} \beta L_0 + \pi \beta^2 t; & t \in [0, H/\beta) \\ 2\beta^2 t \sin^{-1}(H/\beta t); & t \in [H/\beta, W/\beta) \\ 2\beta^2 t [\sin^{-1}(H/\beta t) - \cos^{-1}(W/\beta t)]; & t \in [W/\beta, (H^2 + W^2)^{1/2}/\beta) \\ 0; & t \geq (H^2 + W^2)^{1/2}/\beta \end{cases} \quad (17)$$

where  $L_0$ ,  $H$ , and  $W$  are as shown in Fig. 1. Figure 2 compares this exact measurement to the values predicted by a level set simulation with  $\beta = 1$ . The differences are due to the crude methods used in this preliminary study to extract the length of the level set from the level set function. The “numerical noise” in the predicted values is due to discretization effects. There is room for considerable improvement, using more sophisticated interpolation techniques.

The remainder of this paper concerns the construction of an estimator that will track the evolving feature morphology, based on the total etch rate measurement. The overall strategy is shown in Fig. 3. The level set simulation plays the role of the plant model, and the etch rate  $\beta$  is used as an adjustable parameter. We assume that the initial geometry is known exactly, but that the etch rate, though constant or slowly varying, is not known. The box labeled “G-N” in Fig. 3 represents an algorithm, one possible choice of which is discussed

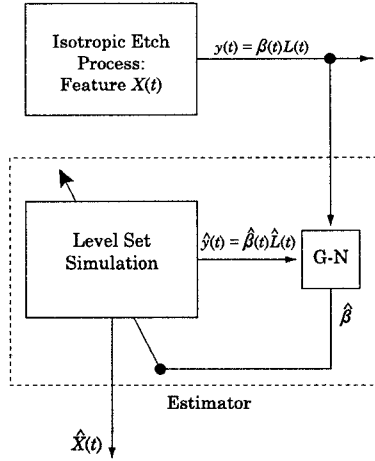


Figure 3: Estimator Structure

below, that solves the inverse problem of “best” matching an etch rate estimate to the measured data. The estimated etch rate is then used to propagate the estimated feature. For our present purpose, “best” will be in a least squares sense.

We express the inverse problem as a minimization,

$$\min_{\beta} J(\beta) = \min_{\beta} \frac{1}{2} \sum_i (\beta L(t_i; \beta) - y(t_i))^2 \quad (18)$$

$$= \min_{\beta} \frac{1}{2} R(\beta)^t R(\beta) \quad (19)$$

where  $[R(\beta)]_i = \beta L(t_i; \beta) - y(t_i)$ . A Newton or Gauss-Newton method would be a standard choice to solve this problem. Here that is not straightforward, because it is not clear how to take derivatives through the set operation in (11). We now show how the necessary derivatives can be obtained.

Following the Gauss approximation to the Hessian often used in least-squares problems,

$$J(\beta)_{\beta} = R(\beta)^t \nabla R(\beta) \quad (20)$$

$$J(\beta)_{\beta\beta} = \nabla R(\beta)^t \nabla R(\beta) + R(\beta)^t \nabla^2 R(\beta) \quad (21)$$

$$\approx \nabla R(\beta)^t \nabla R(\beta) \quad (22)$$

The necessary derivative is given by,

$$[\nabla R(\beta)]_i = L(t_i; \beta) + \beta L_{\beta}(t_i; \beta). \quad (23)$$

At any time  $t_i$ , given some value of  $\beta$ ,  $L(t_i; \beta)$  can be found using a forward solve. It remains to find  $L_{\beta}(t_i; \beta)$ . From [9],

$$L_t(t; \beta) = \beta \int_0^1 \kappa \rho dp = \beta K(t; \beta) \quad (24)$$

Then,  $L_{\beta t}(t; \beta) = L_{t\beta}(t; \beta) \approx K(t; \beta)$ . The total curvature is independent of  $\beta$ , and the approximation above

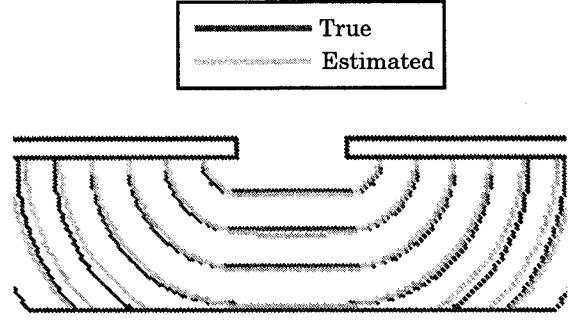


Figure 4: Feature Evolution: Estimated vs True

is exact, when the exposed silicon surface meets the mask or substrate at a right angle. So,

$$L_{\beta}(t_i; \beta) \approx \int_0^{t_i} K(t; \beta) dt. \quad (25)$$

This expression is now applied throughout the etch. The total curvature is generated at any time, for a given value of  $\beta$ , via a forward solve. The surface at  $t_0 = 0$  is assumed known. Then a Gauss-Newton algorithm can be applied to find the surface at any subsequent time. The same technique could be used in a batch mode for run-to-run control of process parameters.

This method was applied to the simplified 2-D etch. Figure 4 shows the surface evolution at 10-unit time intervals. The estimator tracks the surface extremely well through the first part of the etch, before the surface reaches the substrate. After that, the performance is degraded, due to the intersection of the active surface with the substrate at a non-right angle. The correction term for the total curvature due to this effect is easily calculated. However, there are some challenging problems associated with applying the correction term, involving accurate numerical computation of the local curvature and surface normal.

### 3.2 Extensions

As a final note, we comment on two interesting extensions of the problem presented above.

The measurement  $y(t)$  was assumed to be equal to the rate of material removal of the etch. In fact, the measurement is only *proportional* to the total etch rate; and the constant of proportionality must be determined in a separate calibration step. In an industrial setting it is desirable to minimize such steps, which add downtime and increase operating costs. Denote the constant of proportionality by  $\alpha$ . Then the estimated measurement is given by  $\alpha\beta L(t; \beta)$ . To see that this constant can be estimated *simultaneously* with  $\beta$ , consider the exact solution for the first stage of the

etch,  $y(t) = \alpha\beta L(t; \beta) = \alpha\beta(L_0 + \beta\pi t)$ , with  $\alpha$  and  $\beta$  unknown. The measurement will be a straight line,  $y(t) = A + Bt$ . Then  $A$  and  $B$  can be found by a simple linear regression, and  $\alpha$  and  $\beta$  will be given by,  $\beta = BL_0/A\pi$  and  $\alpha = A/\alpha L_0$ . For the general problem, where no exact solution is available, the problem is solved by adding  $\alpha$  to the parameter vector in the Gauss-Newton routine.

Next, we note that there is an alternative to Eq. (24) for calculating the sensitivity. The length of the etching surface may be written as an integral over the entire domain  $\Omega$  [17, 23],

$$L(t) = \int_{\Omega} \chi_{\epsilon} \delta(\Phi) \|\nabla\Phi\| dA \quad (26)$$

where  $\delta$  is the Dirac delta function. Here the  $\beta$  dependence is entirely contained in the dynamics of  $\Phi$ . Unlike Eq. (16), differentiating this expression for  $L$  does not require direct use of the set operation Eq. (11). However, the derivative with respect to  $\beta$  will involve  $\Phi_{\beta}$  and its spatial derivatives. To apply this approach, the sensitivity function  $\Psi := \Phi_{\beta}$  must be found by solving an additional coupled PDE.

### References

- [1] D. Adalsteinsson and J. A. Sethian, "A level set approach to a unified model for etching, deposition, and lithography I: algorithms and two-dimensional simulations," *J. Comp. Physics*, **120**:128–144, 1995.
- [2] S. W. Butler, K. J. McLaughlin, T. F. Edgar, and I. Trachtenberg, "Development of techniques for real-time monitoring and control in plasma etching, II: multivariable control system analysis of manipulated, measured, and performance variables," *J. Electrochem. Soc.*, **138**:9, pp. 2727–2735, 1991.
- [3] L. C. Evans and J. Spruck, "Motion of Level Sets by Mean Curvature. I," *Journal of Differential Geometry*, **33**, pp. 635–681, 1991.
- [4] M. Gage and R. S. Hamilton, "The heat equation shrinking convex plane curves," *J. Differential Geometry*, **23**, pp. 69–96, 1986.
- [5] M. Grayson, "The heat equation shrinks embedded plane curves to round points," *J. Differential Geometry*, **26**, pp. 285–314, 1987.
- [6] I. Katardjiev, G. Carter, and M. Nobes, "The application of the Huygens principle to surface evolution in inhomogeneous, anisotropic and time-dependent systems," *J. Phys. D: Appl. Phys.*, **22**, pp. 1813–1824, 1989.
- [7] S. Kichenassamy, A. Kumar, P. Olver, A. Tannenbaum, A. Yezzi, "Riemannian metrics and geometric active contour models," to appear in *Journal for Rational Mechanics and Analysis*.
- [8] B. B. Kimia, A. Tannenbaum, and S. W. Zucker, "Shapes, shocks, and deformations, I," *Int. J. Computer Vision*, June 1995.
- [9] B. B. Kimia, A. Tannenbaum, and S. W. Zucker, "On the evolution of curves via a function of curvature, I: the classical case," *J. of Math. Analysis and Applications*, **163**, pp. 438–458, 1992.
- [10] R. J. LeVeque, *Numerical Methods for Conservation Laws*, Birkhäuser, Boston, 1992.
- [11] K. J. McLaughlin, S. W. Butler, T. F. Edgar, and I. Trachtenberg, "Development of Techniques for Real-Time Monitoring and Control in Plasma Etching, I: Response Surface Modeling of CF<sub>4</sub>/O<sub>2</sub> and CF<sub>4</sub>/H<sub>2</sub> Etching of Silicon and Silicon Dioxide," *J. Electrochem. Soc.*, **138**:3, pp. 789–798, 1991.
- [12] S. Osher, "Riemann solvers, the entropy condition, and difference approximations," *SIAM J. Numer. Anal.*, **21**, pp. 217–235, 1984.
- [13] S. J. Osher and J. A. Sethian, "Fronts propagation with curvature dependent speed: Algorithms based on Hamilton-Jacobi formulations," *J. Comp. Physics*, **79**, pp. 12–49, 1988.
- [14] B. A. Rashap, M. E. Elta, H. Etemad, J. P. Fournier, J. S. Freudenberg, M. D. Giles, J. W. Grizzle, P. T. Kabamba, P. P. Khargonekar, S. Lafortune, J. R. Moyne, D. Teneketzis, and F. L. Terry, "Control of semiconductor manufacturing equipment: real-time feedback control of a reactive ion etcher," *IEEE Trans. Semiconduct. Manufacturing*, **8**:3, pp. 286–297, 1995.
- [15] J. A. Sethian, "Curvature and the evolution of fronts," *Commun. Math. Physics*, **101**, pp. 487–499, 1985.
- [16] J. A. Sethian, "Numerical Algorithms for Propagating Interfaces: Hamilton-Jacobi Equations and Conservation Laws," *J. Differential Geometry*, **31**, pp. 131–161, 1990.
- [17] J. A. Sethian, *Level Set Methods: Evolving Interfaces in Geometry, Fluid Mechanics, Computer Vision, and Materials Science*, Cambridge University Press, 1996.
- [18] E. Shaqfeh and C. Jurgensen, "Simulation of reactive ion etching pattern transfer," *J. Appl. Physics*, **66**, pp. 4664–4675, 1989.
- [19] V. Singh, E. Shaqfeh, and J. McVittie, "Simulation of profile evolution in silicon reactive ion etching with re-emission and surface diffusion," *J. Vac. Technol. B*, **10**, pp. 1091–1104, 1989.
- [20] J. Smoller, *Shock Waves and Reaction-diffusion Equations*, Springer-Verlag, New York, 1983.
- [21] G. A. Sod, *Numerical Methods in Fluid Dynamics*, Cambridge University Press, Cambridge, 1985.
- [22] A. Srinivasan, C. Batur, B. N. Rosenthal, and W. M. B. Duval, "Solid-Liquid Interface Shape Control During Crystal Growth," *Proc. of the American Control Conference*, Seattle, WA, pp. 1270–1274, 1995.
- [23] M. Sussman, P. Smereka, and S. Osher, "A Level Set Approach for Computing Solutions to Incompressible Two-Phase Flow," *J. Comp. Physics*, **114**, pp. 146–159, 1994.